



Key issues for improving the design and operation of spiral-wound membrane modules in desalination plants

Anastasios J. Karabelas

Laboratory of Natural Resources and Renewable Energies, Chemical Process and Energy Resources Institute (CPERI), Centre for Research and Technology-Hellas (CERTH), 6th km Charilaou-Thermi Road, Themi-Thessaloniki, GR 57001, Greece
Tel. +30 2310498181; Fax: +30 2310498189; email: karabaj@cperi.certh.gr

Received 10 December 2012; Accepted 24 March 2013

ABSTRACT

Spiral-wound membrane (SWM) modules are the most important components of reverse osmosis and nanofiltration desalination and water treatment plants; their optimum design and operation is crucial for achieving satisfactory membrane plant efficiency associated with reduced product cost and environmental impact. This paper is focused on: (a) the main SWM module *design parameters*, in need of optimization, which include the geometrical characteristics of retentate-side spacers and the membrane sheet dimensions (for a module of fixed total active surface area); (b) the major *operating variables*, i.e. the permeate flux and the cross-flow velocity at the retentate side. Membrane element problems, usually encountered in operating plants and affected by the above SWM element parameters, include *membrane fouling* by various species (commonly organic matter, inorganic colloids, and bio-foulants), *membrane scaling* due to sparingly soluble salts, increased *friction losses* and *uneven flow distribution* in the SWM channels. A brief review is presented of the fluid dynamics and mass transfer in spacer-filled narrow channels, stressing the strong interrelation of SWM design and operating parameters. Moreover, the direct effect of the main SWM design and operating parameters on the above membrane element problems is highlighted and quantified, to the possible extent; the impact of these parameters on the efficient plant performance is also outlined. Significant *R* and *D* results are summarized, including currently favoured research approaches for tackling the complicated problem of optimizing desalination SWM module and overall plant performance.

Keywords: Spiral-wound membrane modules; Desalination; Design and operating parameters; Optimization; Operating problems

1. Introduction

1.1. Background

In pursuing improvements of membrane-based water desalination and purification, there are two

general targets; i.e. reduction in product water unit cost and mitigation of environmental impact. To meet these targets four major technical/economic requirements must be met, comprising reduction in plant capital expenses, improvement of energy efficiency, reduction

This paper is based on edited material presented at the *IWA Conference on Wastewater Purification and Reuse*, Heraklion, 28–30 March 2012. Session: Desalination–New Trends and Technological Advances

of chemicals used and increase of membrane life. In fact, several studies (e.g. [1]) have shown that energy and capital expenses constitute a very large percentage (approx. 80%) of the product water unit cost. Energy, chemicals, and membranes, in addition to the operating cost contribution, generally have an adverse environmental impact. Meeting all the above requirements depends to a large extent on the optimum design and performance of SWM modules, which are the main components of the desalination plant.

The established compact design of SWM modules allows packing a large membrane surface area per unit volume. However, this compact design characterized by very narrow spacer-filled channels (of gap less than 1 mm at the retentate side) tends to aggravate operating problems (i.e. friction losses, membrane fouling, and scaling); moreover, it creates serious complications in *R* and *D* efforts to study in detail and understand the module performance which is necessary for improving SWM key features. In particular, detailed/local noninvasive measurements inside the modules are almost impossible to make, thereby depriving researchers and technology developers of essential information. These difficulties have a significant impact on the research approaches taken in SWM studies, rendering theoretical modeling efforts indispensable in connection with idealized experiments in simplified geometries which mimic SWM modules. The flow characteristics and transport properties, inside the narrow SWM channels, determine module performance and they are directly affected by the aforementioned design and operating parameters.

1.2. Main SWM design characteristics, operating parameters, and related problems

A schematic diagram of a typical SWM module [2] is shown in Fig. 1. The currently used standard eight-inch elements are approximately 1 m (40 in.) long. However, there is no standard width of the membrane sheets; i.e. in several well-known commercial modules this width is in excess of 1 m (~1.2 m) and in some other less than 1 m. A membrane envelope is made of two sheets, glued at the three edges, with a cloth filling the permeate channel. The open permeate side of this envelope is fixed on a perforated inner tube where the permeate is collected. Several envelopes, separated by relatively thin net-type spacers, are tightly wrapped around the perforated inner tube. The spacer-filled narrow channels, where the high pressure feed and retentate flow, are the key feature of the SWM modules, playing a very important role in the filtration process, as will be subsequently described.

Major membrane module *design characteristics*, in need of improvement and/or optimization, include

- the physico-chemical characteristics of membrane active surface,
- the geometrical characteristics of retentate-side spacers and
- the membrane sheet dimensions, for a module of fixed total active surface area.

Major *operating parameters*, necessitating optimal selection, are

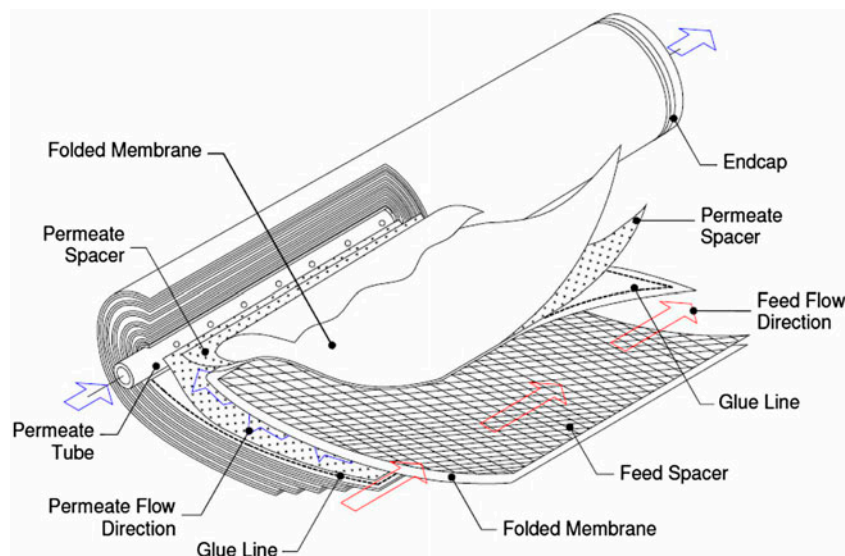


Fig. 1. A view of the SWM module for desalination, showing its configuration (From Johnson and Busch [2], with the authors' permission).

- the permeate flux and
- the cross-flow velocity at the retentate side.

SWM element problems, usually faced in operating plants, comprise

- membrane fouling by various species including organic matter, inorganic colloids, and bio-foulants,
- membrane scaling due to sparingly soluble salts, notably CaCO_3 , and CaSO_4 ,
- increased frictional pressure losses,
- uneven flow distribution in the narrow channels.

Reviewing recently the state of the art in desalination, Elimelech and Phillip [3] concluded that membrane fouling is the most serious problem (impacting on energy consumption, capital cost and the environment), which "... requires the development of fouling resistant membranes with tailored properties, as well as membrane modules with improved hydrodynamic mixing" [3]. This rather comprehensive paper included a review of research efforts to develop improved membranes, but did not deal with issues related to module design and operation.

An inherent difficulty in designing and optimizing desalination plants is the significant increase of retentate salinity and the concomitant reduction of retentate flow rate along the multielement pressure vessels, due to permeate withdrawal. In addition to this axial variability of retentate properties, the local filtration conditions (and in particular the transmembrane pressure, TMP) throughout the membrane sheets of each SWM module are nonuniform. Therefore, to be able to tackle the problem of desalination plant design and optimization at the scale of a multielement pressure vessel, one should first develop an adequate understanding of phenomena taking place *locally* within each SWM element.

This paper aims to highlight the direct effect of the main SWM module design characteristics and operating parameters on the aforementioned problems (i.e. fouling, scaling, pressure drop, and flow distribution) as well as their impact on the technical/economic requirements for efficient and environmentally acceptable plant performance. An overview is presented of recent significant R and D results and of currently favoured approaches for tackling the above problems. Research priorities emerging from this review are outlined.

2. Impact of SWM element design and operating parameters on the main problems

2.1. Transport phenomena in spacer-filled channels

Results will be summarized from comprehensive studies aimed to obtain an improved understanding

of transport phenomena in SWM elements, and to assist in optimizing spacer design (by identifying geometries associated with sufficiently high mass transport coefficients at relatively low pressure drop). The spacers considered consist of two arrays of parallel unwoven thin cylindrical filaments, which intersect at a certain angle, β , and are in contact with both channel walls which represent the membranes, as shown in Fig. 2. This geometry closely resembles currently used commercial spacers within the feed-side SWM channels. The flow field and mass transfer in such complicated narrow passages is influenced by physical and geometrical parameters such as the Reynolds and Schmidt numbers, cylindrical filament diameter D , distance between the filaments L , their intersection angle β , and the angle of flow orientation α .

Significant previous studies (i.e. Li et al. [4,5], Karode and Kumar [6], Geraldies et al. [7], Da Costa et al. [8,9], Fimbres and Wiley [10]) have been complimented and extended by work in this laboratory. Specifically, 2D (Koutsou et al. [11]) and 3D (Koutsou et al. [12]) *direct numerical simulations* of the fluid flow were performed, as well as 3D simulations of the mass transfer (Koutsou et al. [13]) in a rather broad geometrical parameter space. In conjunction with the numerical studies, a significant amount of measurements were obtained of pressure drop and space-averaged mass transfer coefficients for comparison with the theoretical predictions. These data from simulations and experiments (including generalized correlations for various spacer geometries), provide valuable insights into the flow field and mass transfer, and are helpful in efforts to optimize the spacer geometrical characteristics and the performance of SWM elements. In the following, the main results are summarized.

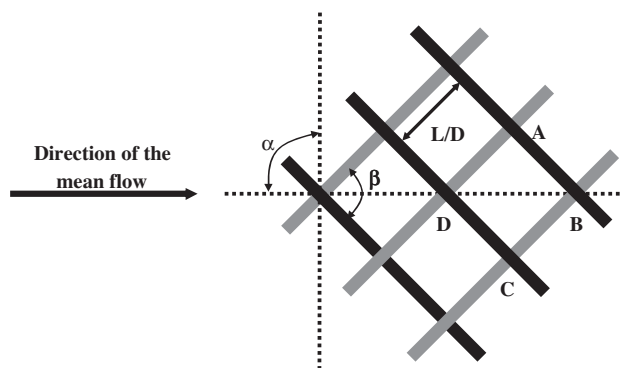


Fig. 2. The geometrical characteristics of a net-type spacer; top view.

2.1.1. Flow field geometry—results of numerical simulations

The flow geometry considered is a close approximation of the narrow spacer-filled channels which are formed in SWM elements; i.e. a flat narrow channel in which a net is placed, comprised of two layers of non-woven straight cylindrical filaments of diameter D . The channel height (H) is twice the cylinder diameter ($H=2D$). In Fig. 2, a top view of the spacer is provided. The main spacer geometrical parameters include the ratio of the distance between parallel filaments to the filament diameter (L/D), and the angle between the crossing filaments β . For reasons outlined by Koutsou et al. [12], the flow attack angle α is taken equal to 90° . It is considered that the flow field exhibits a periodicity based on a unit cell, which is formed by four neighboring cylindrical filaments (indicated as ABCD in Fig. 2); therefore, the flow is studied in this unit cell (a parallelepiped, Fig. 3) that includes half of each of the four cylinders, in which periodic boundary conditions are applied. In commercial spacers the ratio L/D usually varies between 7 and 9, whereas the angle β is in the range of 60° – 120° (Shock and Michel [14], Da Costa et al. [8,9], Zimmerer and Kottke [15]); in most commercial elements $\beta=90^\circ$. In recent years, two types of net-type spacers are used by most major SWM manufacturers, commonly referred to as “28 mil” and “34 mil” spacers (Bartels et al. [16]), which are comprised of unwoven filaments crossing at a $\beta=90^\circ$ angle. The former are thinner (~ 0.028 in., ~ 0.7 mm) and relatively dense; the latter are thicker (~ 0.034 in., ~ 0.86 mm) and less dense. The spacer types studied in detail ([12],[13]) with close correspondence to the above commercial spacers, are characterized by the geometric parameters $L/D=8$, $\beta=90^\circ$ (very similar to “28 mil”), and $L/D=12$, $\beta=90^\circ$ (very similar to “34 mil”).

It should be noted that in this work the angle β is taken equal to or larger than 90° , because when the filament orientation tends to become parallel to the mean flow direction (i.e. $\beta < 90^\circ$) inferior mass transfer performance is obtained, namely smaller mass transfer coefficients, as suggested by several previous experi-

mental (Da Costa et al. [8] and Zimmerer and Kottke [15]) and theoretical studies (Li et al. [4]). The channel walls are considered to be impermeable since the reverse osmosis (RO) permeation velocities are much smaller than the feed flow velocities, justifying this assumption. In addition, for the mass transfer simulations, channel walls are assumed to be of uniform wall concentration, C_w . More details regarding the periodic fluid flow and mass transfer simulations are provided elsewhere (Koutsou et al. [12,13]). The physical parameters of the fluid flow and mass transport in spacer filled channels, are the Reynolds, Schmidt and Sherwood numbers defined as follows.

$$\text{Re} = \frac{U \cdot D}{\nu}, \quad \text{Sc} = \frac{\nu}{D}, \quad \text{Sh} = \frac{k \cdot D}{D}$$

where U : mean superficial velocity in the retentate channel (m/s); D : spacer filament diameter (m); ν : water kinematic viscosity (m^2/s); D : salt diffusivity (m^2/s); k : mass transfer coefficient (m/s)

In practice, the superficial velocity U does not exceed 0.4 m/s and the allowable pressure drop, as recommended by manufacturers, should not exceed 0.6 bar/m (Hydranautics, [17]). In fact, in sea- and brackish-water desalination plants, the superficial velocity at the retentate channels usually varies in the range from ~ 0.10 to ~ 0.20 m/s (Hydranautics [17] and Bartels et al. [16]) depending on the position of an element in the pressure vessel and the particular plant design. The highest velocities are encountered in leading SWM elements of a vessel, with a downstream reduction due to retentate volume decrease. Therefore, the Reynolds number, defined on the basis of the superficial velocity U and the spacer filament diameter D , is less than 200. Typical Schmidt numbers for brackish and sea water are of the order 10^3 .

2.1.2. Pressure drop

Pressure drop in spacer-filled channels, which is partly responsible for the energy expenditure in membrane operations, depends both on the ratio L/D and the angle β between spacer filaments; specifically, pressure drop tends to decrease with increasing ratio L/D and to increase with increasing angle β . For geometries which differ in both the ratio L/D and angle β , pressure drop is found to be larger for the geometry with the smaller ratio L/D . In Fig. 4 the computed dimensionless pressure drop, defined as $\langle \frac{\Delta P}{\Delta L} \rangle = \frac{\Delta P}{\Delta L} \cdot \frac{D}{U^2 \rho}$, is shown to be a rather weak function

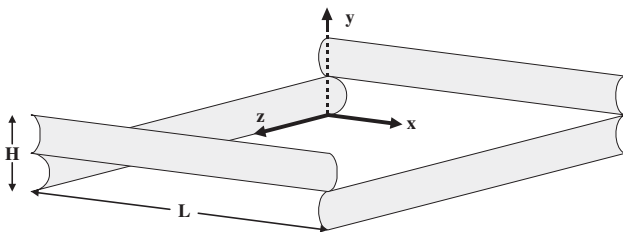


Fig. 3. The geometry for the 3D numerical simulations of the flow field and mass transfer.

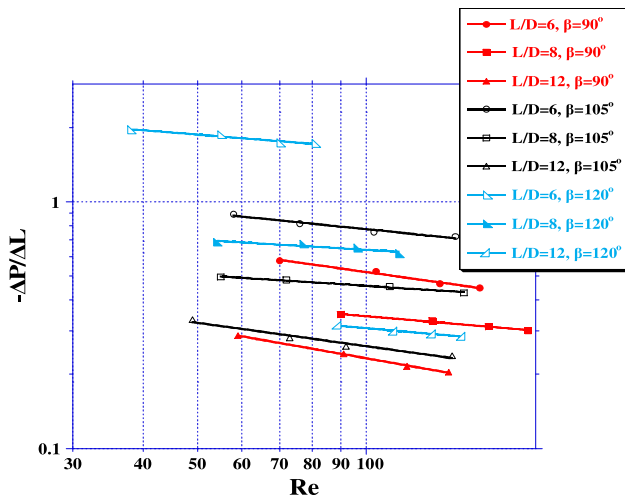


Fig. 4. Calculated dimensionless pressure drop as a function of Reynolds number for several spacer geometries [12].

of Reynolds number, to a power 0.2–0.3, in most cases; corresponding pressure drop correlations are presented elsewhere (Koutsou et al. [12]). The theoretical predictions of pressure drop were compared with experimental data obtained in this work [12], as well as with experimental and theoretical results from the literature, and good agreement was observed. These results show that the pressure drop in spacer-filled channels depends on the superficial flow velocity U to a power around 1.75, and on the H (or filament diameter D) to a power -3 . These dependencies (especially the latter) are strong, with very significant practical implications, as subsequently discussed.

2.1.3. Local wall shear stresses and mass transfer coefficients

The results of the numerical simulations reveal the significant influence of spacer geometry on the local shear stresses and mass transfer coefficients at the membrane surface. Fig. 5(a) and (b) includes the theoretically determined [12] distributions of local shear stresses at the channel/membrane surface, at typical Reynolds numbers, for two spacer types. The detailed flow field characteristics leading to these distributions are presented and analyzed elsewhere [12]. It is evident that shear stresses for the “dense” geometry with $L/D=8$ (Fig. 5(a)) are shifted towards the higher values with a reduced percentage of small or zero values compared to the “less dense” geometry with $L/D=12$ (Fig. 5(b)). In general, the spatial shear stress distributions are quite nonuniform, and there is no tendency for uniformity of the shear field with increasing

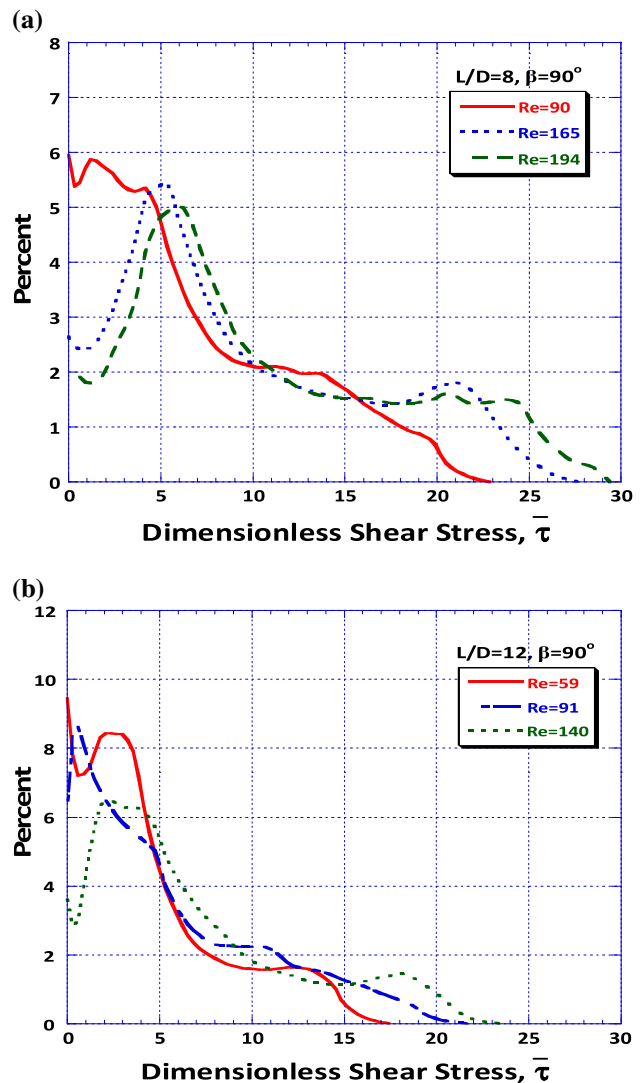


Fig. 5. Predicted [12] distribution of dimensionless wall shear stress for various Reynolds numbers. Spacer geometry characterized by (a) $L/D=8, \beta=90^\circ$ and (b) $L/D=12, \beta=90^\circ$.

cross-flow velocity U ; in fact, it is shown [12] that by increasing Re , the existing at low Re transitional type of flow tends to become rather well developed turbulent above $Re \sim 40$. Fig. 6 presents the effect of the Reynolds number on the dimensionless shear stress $\langle \tau \rangle$, for the spacer geometries of interest ($L/D=8$ and 12 with $\beta=90^\circ$), showing that shear stresses are greater for the “dense” geometry with $L/D=8$. This is in accord with other numerical simulation results showing that the $L/D=8$ spacer geometry exhibits comparatively greater pressure drop (Fig. 4); it will be recalled that a major component of the pressure drop is due to the flat wall shear forces and another due to the spacer. The dimensionless shear stress $\langle \tau \rangle$ is defined as $\langle \tau \rangle = \frac{\tau}{\rho \cdot U^2} Re$.

The data in Fig. 6 are correlated as follows:

$$\langle \bar{\tau} \rangle = 0.42 \cdot \text{Re}^{0.61} \quad (1)$$

for spacer with $L/D = 8, \beta = 90^\circ$

$$\langle \bar{\tau} \rangle = 0.73 \cdot \text{Re}^{0.46} \quad (2)$$

for spacer with $L/D = 12, \beta = 90^\circ$

Eqs. (1) and (2) show that the area-average wall shear stress in the narrow channel with spacers is proportional to the mean superficial cross-flow velocity to an exponent around $n=1.50$. However, in channels without spacers this exponent is $n=1$ for laminar and $n=1.75$ for developed turbulent flow (Dean [18]).

The influence of spacer geometry on the local (time-averaged) Sh number distributions is also

significant. The Sh distributions tend to be displaced towards smaller Sh values as the ratio L/D is increased, and towards higher values as the angle β is increased. Additionally, the local Sh distributions appear to be significantly broader at higher angle β . In Fig. 7, typical images are presented from the simulations of the time-averaged spatial Sh-distributions in comparison with the corresponding shear stresses. This comparison indicates that the mass transfer coefficient and shear stress distributions at the membrane surface are similar, exhibiting extreme (min, max) values almost at the same locations of the unit cell wall. These and other interesting results on local mass transfer rates are presented in detail elsewhere [13].

2.1.4. Average mass transfer coefficients

Fig. 8 includes space average mass transfer measurements [13] obtained with the two prototype spacers considered ($L/D=8, \beta=90^\circ$ and $L/D=12, \beta=90^\circ$) as well as with a commercial 28 mil spacer. It will be noted that the Sh number dependence on Sc (to a power ~ 0.4) has been determined by experiments with fluids of different Sc values. Fig. 8 shows fair agreement of measured average mass transfer coefficients for the 28 mil commercial spacer with those obtained for the prototype spacers, satisfactorily correlated as follows:

$$\langle \text{Sh} \rangle = 0.2 \cdot \text{Re}^{0.57} \cdot \text{Sc}^{0.40} \quad (3)$$

It is interesting that despite the differences in shear stress (of the two spacer geometries considered) the space average mass transfer rates of Fig. 8 are very close. An explanation for this trend is suggested based on the relationship between shear stress τ and mass transfer coefficient k . By comparing the respective correlations (Eqs. (1), (2) with (3)), it is concluded that k is approximately proportional to $\langle \tau \rangle^{1/3}$; therefore, differences that may exist on $\langle \tau \rangle$ (between the two

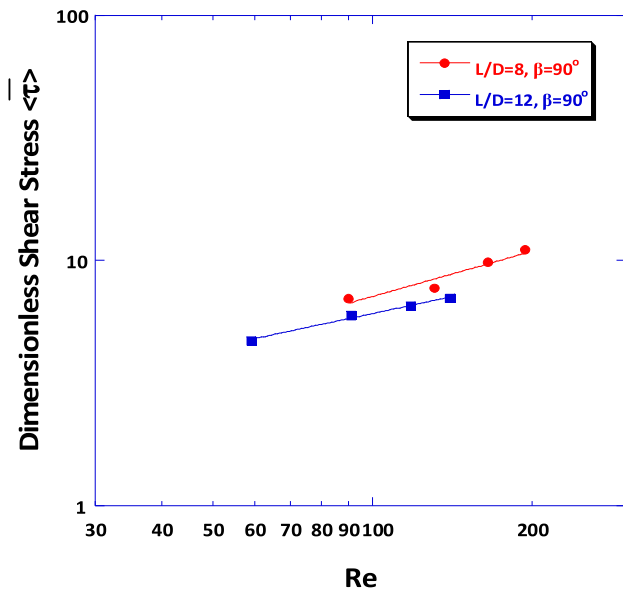


Fig. 6. Effect of Reynolds number on dimensionless average shear stress for two prototype spacer geometries similar to commercial spacers.

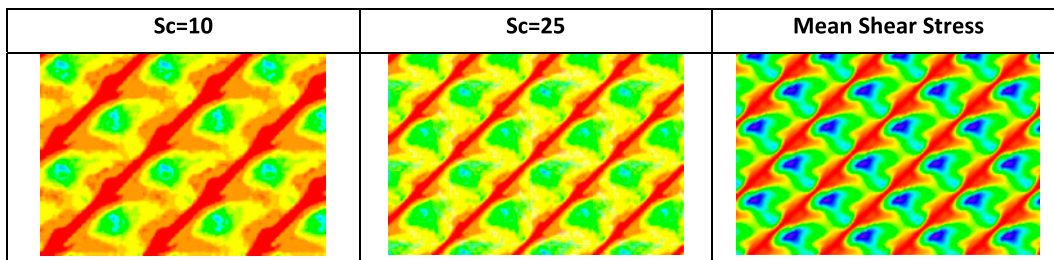


Fig. 7. Distribution of local values of time-averaged mass transfer coefficient and wall shear stress, for the channel top wall (Koutsou et al. [13]). Spacer geometrical characteristics: $L/D=6, \beta=90^\circ$. Mean flow direction from left to right. Red and blue colors correspond to minimum and maximum values, respectively; $\text{Re} = 80$.

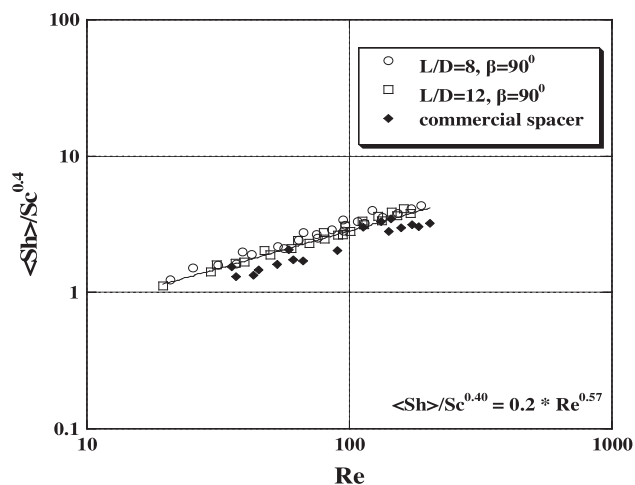


Fig. 8. Measurements of Sh dependence on Re and Sc numbers for the commercial spacer in comparison with data for two custom-made spacers of similar geometry (Koutsou et al. [13]).

spacer geometries) tend to be significantly reduced due to this weak (1/3) power dependence. It is noted that experimental data obtained by Li et al. [5] are in substantial agreement with the above correlation (Eq. (3)), as shown by Koutsou and Karabelas [19].

2.2. Fluid dynamic characteristics throughout membrane sheets in SWM elements

As noted above, the design and optimization of desalination plants is complicated by the very significant axial variability of retentate properties, and by the nonuniform local filtration conditions (in particular the TMP) throughout the membrane sheets of each SWM module, even in the absence of fouling. A relatively recent review (Schwinge et al. [20]) provides a useful summary of several previous SWM simulation efforts. The novel approach outlined here, based on a periodic “unit cell”, appears to be fruitful for modeling the fluid dynamics in SWM. The detailed data obtained on transport phenomena in spacer-filled channels (Section 2.1) allow to tackle the problem at a meso-scale (Kostoglou and Karabelas [21,22]), i.e. at the length scale of the “unit cell”, and further to describe and predict the flow field throughout an entire membrane sheet; this is the basis for developing a simulator for predicting the flow field along an entire multielement pressure vessel. The dynamic model recently developed [22] is not restricted to describing only the fluid mechanical characteristics, but it is structured in such a way as to permit incorporation, in a fundamental manner, of specific (constitutive type) relationships for

modeling other concurrently occurring phenomena (i.e. membrane fouling and scaling).

The comprehensive simulation of the flow field throughout a membrane sheet, including ionic species rejection, is difficult. As a first step, ignoring the feed water ionic strength, progress has been made in modeling this problem and in the development of efficient mathematical solution techniques (Kostoglou and Karabelas [21,22]). This is a necessary step before extending this approach to account for more realistic fluid properties and for membrane fouling and scaling. Nevertheless, realistic results of possible practical significance can be obtained from these models; for instance, it is shown that the pressure at the retentate side essentially varies only in the x -direction (lengthwise), whereas the pressure at the permeate side is only y -dependent. Qualitatively, this trend is attributed to the effect of spacer at the retentate side, which tends to promote fluid dispersion and eliminate lateral pressure variations.

2.3. Membrane fouling and scaling

The phenomena of fouling are quite complicated and the impact of the spacer geometry thereon cannot be easily quantified, although some general (rather qualitative) trends are known in practice and fairly well established in the literature. *Colloidal fouling* by organic and inorganic species is currently a major problem in membrane desalination plants, affected by a multitude of factors, as discussed in relevant reviews (Yiantsios et al. [23], Tang et al. [24]). The direct and indirect effects of spacers and of module operating parameters on colloidal fouling may be summarized as follows:

- Large cross-flow velocities inducing high wall shear stresses are considered beneficial as they tend to reduce the deposition efficiency of various foulants (e.g. Yiantsios and Karabelas [25]). However, during the initial phase of membrane fouling layer formation, which is of practical interest (Sioutopoulos and Karabelas [26]), and within the range of modest cross-flow velocities encountered in practice (commonly 0.1–0.2 m/s) the effect of cross-flow velocity may not be significant, at least for some common classes of foulants including polysaccharides (Lee et al. [27], Sioutopoulos et al. [28,29]). In general, uncertainty exists regarding the relative magnitude of cross-flow velocity effects, for the various foulants present in the feed waters to RO membrane plants; thus, additional research on this topic is required.

- Regions of membrane surface, where small shear stresses (as shown in Fig. 7) or small convective local velocities prevail, appear to be associated with increased local fouling rates; this effect is greater in membrane regions close to contact lines between spacer filaments and membrane, as already observed in the laboratory (e.g. Koutsou et al. [13]; pictures in Figs. 12 and 13), leading to spatial fouling layer non-uniformity. The above mentioned quite extensive results, relating the spacer geometrical parameters with the narrow channel hydrodynamics, provide guidance for additional R and D work to optimize the spacer characteristics aimed at mitigating fouling.
- Generally, permeate flux has a significant direct effect on fouling [23], although this issue has not been clarified in the literature yet [24]. Significant uncertainty on this effect exists partly because the great majority of relevant laboratory tests is performed under constant filtration pressure, and therefore variable/decreasing flux due to fouling; indeed, fouling data under constant flux are very meagre, as these tests are somewhat more difficult to perform compared to those at constant pressure. Only very recently Sioutopoulos and Karabelas [26] showed that, for the case of RO or UF membrane organic fouling, the specific fouling layer resistance α , obtained under conditions of constant flux and constant pressure, can be satisfactorily correlated if plotted versus the pressure drop across the fouling layer/cake thickness ΔP_c . This successful correlation can lead to a generalized expression relating the fouling resistance α to the permeate flux J ; a rather strong dependence of α on J to a power between 1.5 and 1.8 is determined for typical organic foulants comprising a significant percentage of polysaccharides. Expressions of this type (i.e. α as a function of J) are necessary to model and predict the spatial and temporal evolution of fouling throughout a SWM element, as outlined in the preceding section and recently shown by Kostoglou and Karabelas [30]. In the latter, a mathematical model formulated in a fundamental manner, takes into account the spatial flow field nonuniformities inside spacer-filled narrow channels and their interaction with the evolving deposits; the cases of constant inlet pressure and constant average permeate flux are treated. A problem analysis has guided the development of efficient numerical techniques, considered useful for future extensions towards the development of a comprehensive modeling tool, appropriate for module design calculations and for assessing detailed experimental data. Fig. 9(a) and (b), including typical distributions of normalized foulant mass $M = m/m_{av}$ on a

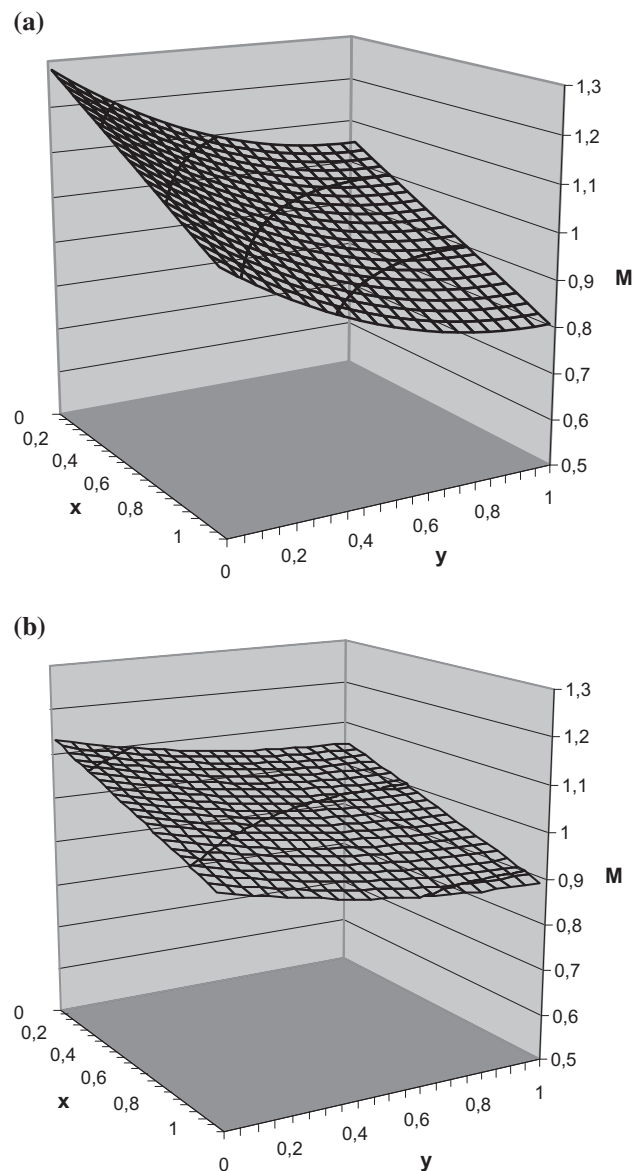


Fig. 9. Predicted two-dimensional spatial profiles of normalized deposit mass $M = m/m_{av}$ throughout a membrane sheet in a spacer-filled narrow channel, simulating SWM module operation, at times (a) $t=0$ (start of operation) and (b) $t=2$. Computations (Kostoglou and Karabelas [30]) with parameters $B=0.5$, $A=0$, $p_o=0.8$, considering an organic membrane fouling model.

membrane sheet, demonstrate the potential of this modeling approach; these distributions correspond to clean (time $t=0$, Fig. 9(a)) and fouled (dimensionless time $t=2$, Fig. 9(b)) membranes. The graphs show that an initial nonuniformity of the mass density distribution throughout a membrane sheet (Fig. 9(a)), tends to be reduced with time (leading to a “smoothing”, Fig. 9(b)), which appears to be a notable outcome of the dynamic interaction

of the deposition process with the flow fields at both sides of the membrane.

The effect of spacers on *membrane scaling* due to sparingly soluble salts (CaCO_3 , CaSO_4 , etc.), has been much less studied; indeed, detailed data are very limited on the onset and development of inorganic scale within a SWM element, which are caused by supersaturation of such salts *at the membrane surface* due to desalination. With the exception of a very recent study [31], only indirect information on scaled membranes is available, mostly from autopsies of SWM withdrawn from operating or pilot plants. Evidence derived from both dead-end [32] and cross-flow desalination experiments [31] as well as theoretical modeling [33] suggest that the increased salt supersaturation at the membrane surface, due to desalinated water permeation, tends to promote nucleation of crystals (e.g. CaCO_3 , CaSO_4) thus playing a significant role in the scaling process. Membrane surface supersaturation ratio, S_w , as discussed above and elsewhere [31] in more detail, is affected by both permeate flux J and retentate velocity. S_w is enhanced by the flux J , but tends to be reduced by increased cross-flow velocity and the concomitant increase of shear stresses τ and mass transfer coefficients k at the membrane surface; τ and k are significantly affected by retentate-side spacers, as outlined in preceding sections. Therefore, the spacers affect membrane scaling, at least indirectly. Relevant is the study by Chai et al. [34] who ran pilot tests of CaSO_4 scaling with a SWM module and found (by an autopsy) uneven scale distribution on membrane sheets, with greater deposit mass near the permeate collection tube; this trend may be related with the nonuniform TMP distribution, as this is the membrane area of relatively greater local TMP and flux J [22].

The negative economic and environmental implications of membrane fouling and scaling are well-known and can be quantified by considering the frequency of cleaning the membranes to restore their performance, the chemicals used, the productivity reduction due to plant downtime and the related spent-water disposal (e.g. Wilf [35]). Moreover, frequent chemical cleaning of membranes accelerates their degradation, and shortens their useful life, thereby increasing the cost associated with module replacement. The related negative environmental impact is obvious. As discussed above, permeate flux J and cross-flow velocity U are the main operating parameters affecting membrane fouling/scaling; in turn, J and U are influenced directly and indirectly by spacer-filled channel design parameters. Therefore, the selection of optimum flux J and cross-flow velocity U should be made in relation to the spacer geometrical parameters.

3. Towards optimization of SWM design and operation

3.1. General considerations

The *membrane surface physico-chemical properties*, which is one of the main SWM design characteristics, will not be dealt with in this paper; a fairly thorough review of related research efforts is presented by Elimelech and Phillip [3]. The “optimization” of *membrane sheet dimensions* (for a module with fixed external dimensions and total active membrane surface area) is currently done in industry in a rather empirical manner. It has been already shown in practice that a greater number of membrane envelopes (of reduced width) may be preferable in comparison to a relatively smaller number of wider sheets (Lomax [36]); this is attributed to the reduced pressure drop, necessary to drive the permeate towards the permeate inner tube, in the former case. Support for this argument can be obtained from modeling and theoretical predictions of the flow field (Schwinge et al. [20], Kostoglou and Karabelas [22]). However, a sound optimization effort (including concentration polarization effects, membrane sheet dimensions, and fouling evolution) should await the development of a comprehensive global SWM simulation tool.

In attempts to determine an *optimum* (or near-optimum) *spacer geometry*, one should take into consideration the effects of three parameters; i.e. *feed flow pressure drop* which directly affects energy expenditure, *mass transfer rates* of dissolved species to the wall which strongly influence concentration polarization, and *shear stresses* at the membrane surface; the latter, as discussed, affect membrane fouling and scaling. Spacer optimization should be based on quantitative criteria concerning the above parameters. These issues of spacer geometry optimization are discussed by Koutsou and Karabelas [37], by taking into account the numerical simulation results outlined in Section 2.1. It is suggested that the computed parameters of pressure drop and mass transfer coefficients can be utilized for the assessment of various spacer geometries, in a quantitative manner. Criteria, essentially qualitative, relating wall shear stresses to spacer geometries, as discussed above, could supplement the above computational results of pressure drop and mass transfer. It is also argued that the “optimum” spacer geometry depends on the kind of membrane process considered (i.e. RO or nanofiltration), in relation to the specific properties of the feed water, which implies that very likely there exists no single spacer geometry with universally optimum characteristics. Furthermore, Koutsou and Karabelas [37], based on the numerical simulation results, made an assessment

of trends towards spacer geometry optimization. They concluded that for RO membrane desalination, where pressure drop, shear stresses, and mass transfer rates play a significant role, spacer parameter values that appear to be associated with improved element performance are near $L/D=12$ with an angle β closer to 120° than to 90° . Evidently such a preliminary assessment provides only trends, which are subject to verification through further experimentation and numerical simulations. It should be added that in the preceding analysis it has been tacitly assumed that the retentate (and permeate) spacers are incompressible and thus nondeformable during the SWM module fabrication. However, Johnson and Busch [2] report that currently used commercial spacers may be compressed if the number of contact points/regions (per unit membrane area) between membrane and spacer is not sufficiently large. Under such conditions, the effective retentate channel gap would decrease, with obvious negative impact on pressure drop; moreover, an additional element of complication would be introduced in the efforts towards SWM module optimization.

3.2. An example of selecting optimum spacer geometry for RO elements

As discussed, the optimum spacer geometry apparently depends on the kind of membrane process considered, in relation to the specific characteristics of the feed water. Consequently, the issue of the optimum spacer geometry should be examined separately

for each major category of membrane applications. An example is provided here for RO seawater desalination, with a membrane that is not fouled, to demonstrate the usefulness of the numerical results outlined herein. To take into account quantitatively the effect of spacer geometry on both pressure drop and concentration polarization, the following function is considered, in search of an optimum.

$$\frac{\Delta P_{\text{eff}}}{\Delta P_{\text{nominal}}} = \frac{\Delta P_{\text{applied}} - \Delta P_f - CP \cdot \Delta \pi}{\Delta P_{\text{applied}} - \Delta \pi} \quad (4)$$

where: $\Delta P_{\text{applied}}$: the applied transmembrane pressure; ΔP_{eff} : the effective operating pressure difference; ΔP_f : the pressure drop at the feed water channel; CP : the concentration polarization factor; $\Delta \pi$: the osmotic pressure difference; $\Delta P_{\text{nominal}}$ is the difference between the applied pressure and the osmotic pressure computed on the basis of bulk salt concentration, whereas the effective operating pressure difference is further reduced due to pressure drop in the feed channel and the concentration polarization. The latter effect may be quantified, as is common (e.g. Mulder, [38]), by determining a concentration polarization factor $CP = \exp(J/k)$, where J is the transmembrane flux and k the mass transfer coefficient, computed from correlations [13] that depend on the particular spacer geometry. To obtain specific numerical results, the pressure conditions prevailing at the end of the first element in an array

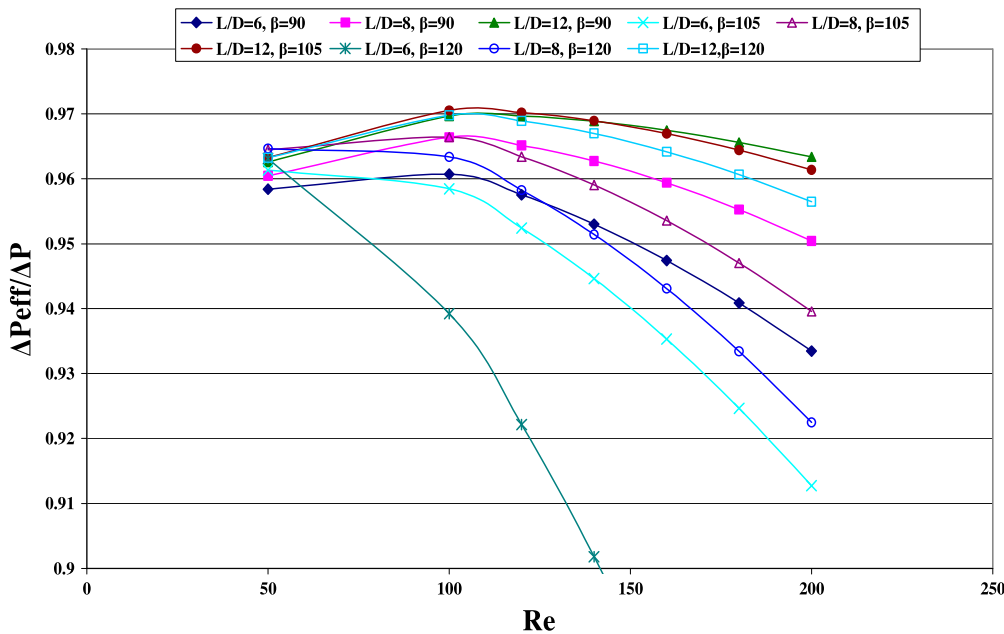


Fig. 10. The ratio of the effective over the nominal TMP as a function of the feed channel Reynolds number (Koutsou and Karabelas [37]).

(i.e. 1.0 m from feed entry) are estimated, for various spacer geometries. Typical process parameter values are employed for seawater of salinity 35,000 ppm NaCl. The case of a typical (e.g. [16]) “34 mil” spacer is considered. Other parameter values used in the calculations are typical for seawater desalination.

In Fig. 10, the ratio of effective over the nominal TMP is plotted as a function of feed channel Reynolds number, for the various spacer geometries examined in this work. Fig. 10 shows that for most spacer geometries there is a rather narrow range of near optimum operation (from the standpoint of effective pressure) characterized by Re numbers roughly 100–120. At Re below 100, the mass transfer rates are relatively small and concentration polarization tends to enhance the effective osmotic pressure at the membrane surface, thus reducing the effective TMP; at Re above 120, pressure drop in the channel due to higher-cross flow tends to become excessive and to eliminate any benefits resulting from the concomitant reduction of concentration polarization. It is further noted that, among the cases considered, spacer geometries with $L/D=12$ exhibit better performance in comparison with the other geometries, i.e. the greatest values of the effective over nominal TMP; this is in accord with the general trends suggested by an overall assessment of the computational results outlined in Koutsou et al. [12]. It should be finally pointed out that the cross-flow velocity corresponding to the Re range 100–120 (where the performance appears to be near optimum) is around 0.25 m/s, that is near the commonly used operating velocities in commercial plants, and recommended by membrane element manufacturers.

4. Concluding remarks

The flow field and transport properties inside the narrow channels of SWM are greatly affected by the geometrical characteristics of retentate side spacers. Advanced Direct Numerical Simulations at the unit cell level, experiments in special test sections and theoretical studies lead to the following conclusions regarding the main design and operating parameters of SWM modules.

The pressure drop $\Delta P/\Delta L$ is affected by the detailed geometrical features of spacers; $\Delta P/\Delta L$ depends on the superficial cross flow velocity to an exponent around 1.50 and on the channel gap $H=2D$ to a power -3 . The latter (very strong) dependence implies that even a relatively small reduction of gap (e.g. due to fouling) can cause a very significant increase of pressure drop; moreover, it suggests that

within the SWM overall size and geometrical constraints, channel gaps as large as possible are desirable. The less dense spacers, e.g. $L/D=12$, are also associated with reduced friction losses, provided they are rigid and not deformable.

Local and average shear stresses and mass transfer coefficients. The spatial distributions of local wall stress τ and mass transfer coefficient k are rather broad, significantly affected by the contact lines of spacer filaments with the membranes. In these regions of membrane surfaces small values of τ and k prevail, which are undesirable. Local shear stresses are generally greater for the more “dense” spacer geometries (i.e. for relatively small L/D). However, somewhat greater wall stresses prevail with increasing angle of filament intersection β . A close similarity of local mass transfer coefficient distributions compared to those of shear stresses is evident, as expected. The aforementioned trends of wall stresses τ as a function of L/D and β are also observed in the case of coefficients k . In general, large values of average \bar{k} and $\bar{\tau}$ are desirable as they are associated with reduced concentration, polarization, and membrane fouling; however, \bar{k} and $\bar{\tau}$ tend to increase with increasing cross flow velocity U to an exponent ~ 0.6 and 1.5 , respectively. If these trends and velocity dependencies (related to \bar{k} and $\bar{\tau}$) are contrasted with the opposite requirements for avoiding increase in friction losses, a genuine optimization problem emerges. A simplified example to demonstrate these opposite trends and to address the optimization of net-type spacer geometrical details, based on minimization of friction losses, is cited [37] indicating that near-optimum SWM element performance may be obtained with superficial cross-flow velocity near 0.20–0.25 m/s, and parameters $(L/D)=12$ and β between 90° and 120° , for gap thickness $H \approx 0.86$ mm (34 mils).

Progress has been made in recent years towards developing comprehensive global models to predict flow parameters as well as the temporal evolution of fouling throughout membrane sheets of SWM modules. The direct numerical simulation results, at the unit cell level, provide the basis for formulating these comprehensive models. However, a considerable amount of work remains to be done, both theoretical and experimental, to further develop and validate such tools, and render them useful for improved module design and operation. An approach to achieve this goal, which is proven quite fruitful so far [22,30] is to improve our understanding of important phenomena (i.e. fouling and, scaling) at the local level, through careful experimentation, and to develop reliable and convenient “computational modules” or submodels

(i.e. a kind of constitutive relations for these phenomena); next, these “modules” should be integrated in a generalized modeling framework, thus allowing predictions of SWM element operation under various conditions as well as SWM performance optimization. The recent introduction into the market of longer, larger (i.e. 16-inch) and more expensive SWM modules, on which insufficient historical data and practical experience exist, underlines the significance and the necessity of these R&D efforts.

Acknowledgments

The author wishes to acknowledge the significant contributions, summarized in this paper, by his former students and present collaborators Prof S.G. Yiantsios, Prof M. Kostoglou, Dr C. P. Koutsou and Dr D. C. Sioutopoulos. Grateful acknowledgement is also made of financial support received by the *Middle East Desalination Research Center (MEDRC)* for part of the work summarized herein.

References

- [1] M. Wilf, C. Bartels, Optimization of seawater RO systems, *Desalination* 173 (2005) 1–12.
- [2] J. Johnson, M. Busch, Engineering aspects of reverse osmosis module design, *Desalin. Water Treat.* 15(1–3) (2010) 236–248.
- [3] M. Elimelech, W.A. Phillip, The future of seawater desalination: Energy, technology and the environment, *Science* 333 (2011) 712–717.
- [4] F. Li, W. Meindersma, A.B. de Haan, T. Reith, Optimization of commercial net spacers in spiral wound membrane modules, *J. Membr. Sci.* 208 (2002) 289–302.
- [5] F. Li, W. Meindersma, A.B. de Haan, T. Reith, Experimental validation of CFD mass transfer simulations in flat channels with non-woven spacers, *J. Membr. Sci.* 232 (2004) 19–30.
- [6] S.K. Karode, A. Kumar, Flow visualization through spacer filled channels by computational fluid mechanics I. Pressure drop and shear stress calculations for flat sheet geometry, *J. Membr. Sci.* 193 (2001) 69–84.
- [7] V. Geraldes, V. Semiao, M.N. de Pinho, Flow management in nanofiltration spiral wound modules with ladder type spacers, *J. Membr. Sci.* 203 (2002) 87–102.
- [8] A.R. Da Costa, A.G. Fane, D.E. Wiley, Spacer characterization and pressure drop modelling in spacer-filled channels for ultrafiltration, *J. Membr. Sci.* 87 (1994) 79–98.
- [9] A.R. Da Costa, A.G. Fane, Net-type spacers: Effect of configuration on fluid flow path and ultrafiltration flux, *Ind. Eng. Chem. Res.* 33 (1994) 1845–1851.
- [10] G.A. Fimbres, D.E. Wiley, Review of 3D CFD modelling of flow and mass transfer in narrow spacer-filled channels in membrane modules, *Chem. Eng. Process.: Process Intensification* 49(7) (2010) 759–781.
- [11] C.P. Koutsou, S.G. Yiantsios, A.J. Karabelas, Numerical simulation of the flow in plane channel containing a periodic array of cylindrical turbulence promoters, *J. Membr. Sci.* 231 (2004) 81–90.
- [12] C.P. Koutsou, S.G. Yiantsios, A.J. Karabelas, Direct numerical simulation of flow in spacer-filled channels: Effect of spacer geometrical characteristics, *J. Membr. Sci.* 291 (2007) 53–69.
- [13] C.P. Koutsou, S.G. Yiantsios, A.J. Karabelas, A numerical and experimental study of mass transfer in spacer-filled channels: Effects of spacer geometrical characteristics and Schmidt number, *J. Membr. Sci.* 326 (2009) 234–251.
- [14] G. Shock, A. Miquel, Mass transfer and pressure loss in spiral wound modules, *Desalination* 64 (1987) 339–352.
- [15] C.C. Zimmerer, V. Kottke, Effects of spacer geometry on pressure drop, mass transfer, mixing behavior, and residence time distribution, *Desalination* 104 (1996) 129–134.
- [16] C. Bartels, M. Hirose, H. Fujioka, Performance advancement in the spiral wound RO/NF element design, *Desalination* 221 (2008) 207–214.
- [17] Hydranautics, IMSDesign® - Hydranautics Membrane Solutions Design Software, v. 2012. Available from www.membranes.com, December 2012.
- [18] R.B. Dean, Reynolds number dependence of skin friction and other bulk flow variables in two-dimensional rectangular duct flow, *Trans. ASME: J. Fluids Eng.* 100 (1978) 215–225.
- [19] C.P. Koutsou, A.J. Karabelas, Shear stresses and mass transfer at the base of a stirred filtration cell and corresponding conditions in narrow channels with spacers, *J. Membr. Sci.* 399–400 (2012) 60–72.
- [20] J. Schwinge, P.R. Neal, D.E. Wiley, D.F. Fletcher, A.G. Fane, Spiral wound modules and spacers. Review and analysis, *J. Membr. Sci.* 242 (2004) 129–153.
- [21] M. Kostoglou, A.J. Karabelas, On the fluid mechanics of spiral wound membrane modules, *Ind. Eng. Chem. Res.* 48 (2009) 10025–10036.
- [22] M. Kostoglou, A.J. Karabelas, Mathematical analysis of the meso-scale flow field in spiral wound membrane modules, *Ind. Eng. Chem. Res.* 50 (2011) 4653–4666.
- [23] S.G. Yiantsios, D.C. Sioutopoulos, A.J. Karabelas, Colloidal fouling of RO membranes—An overview of key issues and efforts to develop improved prediction techniques, *Desalination* 183 (2005) 257–272.
- [24] C.Y. Tang, T.H. Chong, A.G. Fane, Colloidal interactions and fouling of NF and RO membranes, *Adv. Colloid Interface Sci.* 164 (2011) 126–143.
- [25] S.G. Yiantsios, A.J. Karabelas, Deposition of micron-sized particles on flat surfaces: Effects of hydrodynamic and physicochemical conditions on particle attachment efficiency, *Chem. Eng. Sci.* 58 (2003) 3105–3113.
- [26] D.C. Sioutopoulos, A.J. Karabelas, Correlation of organic fouling resistances in RO and UF membrane filtration under constant flux and constant pressure, *J. Membr. Sci.* 407–408 (2012) 34–46.
- [27] S. Lee, W.S. Ang, M. Elimelech, Fouling of reverse osmosis membranes by hydro-philic organic matter: Implications for water reuse, *Desalination* 187 (2006) 313–321.
- [28] D.C. Sioutopoulos, S.G. Yiantsios, A.J. Karabelas, Relation between fouling characteristics of RO and UF membranes in experiments with colloidal organic and inorganic species, *J. Membr. Sci.* 350 (2010) 62–82.
- [29] D.C. Sioutopoulos, A.J. Karabelas, S.G. Yiantsios, Organic fouling of RO membranes: Investigating the correlation of RO and UF fouling resistances for predictive purposes, *Desalination* 261 (2010) 272–283.
- [30] M. Kostoglou, A.J. Karabelas, A mathematical study of the evolution of fouling and operating parameters throughout membrane sheets comprising spiral wound modules, *Chem. Eng. J.* 187 (2012) 222–231.
- [31] S.T. Mitrouli, A.J. Karabelas, A. Karanasiou, M. Kostoglou, Incipient calcium carbonate scaling of desalination membranes in narrow channels with spacers—experimental insights, *J. Membr. Sci.* 425–426 (2013) 48–57.
- [32] A.J. Karabelas, M. Kostoglou, S.T. Mitrouli, Incipient crystallization of sparingly soluble salts on membrane surfaces: The case of dead-end filtration with no agitation, *Desalination* 273 (2011) 105–117.

- [33] M. Kostoglou, A.J. Karabelas, On modelling incipient crystallization of sparingly soluble salts in frontal membrane filtration, *J. Colloid Interface Sci.* 362 (2011) 202–214.
- [34] G.-Y. Chai, A.R. Greenberg, W.B. Krantz, Ultrasound, gravimetric, and SEM studies of inorganic fouling in spiral-wound membrane modules, *Desalination* 208 (2007) 277–293.
- [35] M. Wilf, *Membrane desalination technology*, Balaban Desalination, L'Aquila, 2007.
- [36] I. Lomax, Experiences of Dow in the field of seawater reverse osmosis, *Desalination* 224 (2008) 111–118.
- [37] C.P. Koutsou, A.J. Karabelas, Towards optimization of spacer geometrical characteristics for spiral wound membrane modules, *Desalin. Water Treat.* 18 (2010) 139–150.
- [38] M. Mulder, *Basic principles of membrane technology*, second ed., Kluwer Academic, Dordrecht, 1997.